Node Deployment under Position Uncertainty for Network Localization

Mohammad Javad Khojasteh, Augustin A. Saucan, Zhenyu Liu, Andrea Conti, and Moe Z. Win

***Abstract*—Network localization performance depends on the network geometry and, therefore, node deployment methods are critical for high-accuracy localization. Optimal node deployment is challenging in practical problems due to various uncertainties present in the position knowledge of the deployed nodes. In this paper, we propose a node-deployment method for network localization that accounts for such uncertainties. We develop a framework for the optimal deployment of location-aware networks under bounded disturbances in the positions of the sensing nodes. More specifically, by considering bounded discrepancies in the network geometry, we characterize the optimal deployment according to the D-optimality criterion and assert its implications for the A-optimality and E-optimality criteria. Results show that the proposed optimization-based design achieves a significative improvement according to the D-optimality criterion.**

***Index Terms*—network localization, node deployment, Fisher information, sensor network**

I. Introduction

Location-awareness is vital for the operation of wireless networks and their applications [1]–[3], including factory of the future (FoF) [4]–[6], smart environments [7]–[9], asset tracking [10]–[12], autonomy [13]–[16], crowdsensing [17]–[19], and Internet-of-Things (IoT) [20]–[23]. The localization performance strongly depends on the wireless environment and the network's geometry. In applications such as ocean-of-things (OoT) [24] or indoor positioning [25], due to external disturbances and obstacles, inaccuracies appear between the desired and the actual deployed position of the nodes. These position inaccuracies may also occur in adversarial scenarios such as Internet-of-Battlefield-Things (IoBT) [26], where an adversary aims to hamper the localization process of legitimate nodes by forcing them to move from their initial or desired positions. Therefore, these emerging applications require the investigation of node-deployment methods that account for uncertainties in the positioning of the nodes.

The fundamental limits of network localization and navigation (NLN) provide performance benchmarks and are essential for network design [27], [28]. There are a few criteria for assessing the optimal network geometry that can be written as a function of the eigenvalues of the inverse of the Fisher information matrix (FIM), including A-optimality, D-optimality, and E-optimality criteria [29]–[32]. The D-optimality, A-optimality, and E-optimality criteria correspond to minimizing determinant, trace, and the largest eigenvalue of the inverse FIM, respectively.

The optimal network geometry for high-accuracy localization has been studied in [33]–[38], where the optimal sensor arrangement encircles the target. In many applications, such as radar and sonar, the target is far away from the sensors. In this case, it might not be possible to surround the target with sensors. Hence, the recent work in [32] investigates the case where the sensors' positions might be restricted. The A-optimality, D-optimality, and E-optimality criteria are equivalent for 2-D target localization when the range information intensity (RII) [28] are fixed. In this context, in [32] it was shown that the optimal sensor configuration follows a symmetric pattern with respect to the target of interest. In practical problems, such a pattern is difficult to achieve due to the uncertainty in the positions of deployed nodes. The work in [31] also considers the localization of a single target using two mobile sensors and provides optimal way-points that the moving sensors need to reach. Moreover, the work in [39] studied spatiotemporal signal reconstruction with node position uncertainty. The work in [40] studied the Bayesian Cramér-Rao lower bound for localization and under additive uncertainty in the deployment of sensors. However, optimization-based, robust, and practical node deployment algorithms for the design of location-aware networks are still lacking.

In this paper, we develop a node deployment method for NLN under uncertainty in the positions of the deployed nodes. We employ the criteria of A-optimality, D-optimality, and E-optimality to optimize network geometry in the presence of discrepancies between the desired deployment and the actual positioning of nodes. Our approach is based on optimization theory and sets the basis for the study of *robust* NLN in the presence of uncertainties in the positioning of the nodes. The key contributions of this paper can be summarized as follows:

- we develop a framework for optimal node deployment by introducing the concept of relaxed sensor pairing;
- we characterize upper and lower bounds on functions of FIM corresponding to the D-optimality, A-optimality, and E-optimality criteria; and
- we demonstrate that the optimal design could be obtained via solving a bilinear program.

This research was supported, in part, by the Office of Naval Research under Grants N00014-16-1-2141 and N62909-22-1-2009, and in part by the Army Research Office through the MIT Institute for Soldier Nanotechnologies, under Contract W911NF-13-D-0001. *(Corresponding author: Moe Z. Win).*

M. J. Khojasteh, A. A. Saucan, and Z. Liu are with the Wireless Information and Network Sciences Laboratory, Massachusetts Institute of Technology, Cambridge, MA 02139. E-mails: {mkhojast,asaucan, zliu14}@mit.edu

A. Conti is with the Department of Engineering and CNIT, University of Ferrara, Via Saragat 1, 44122 Ferrara, Italy. E-mail: a.conti@ieee.org

M. Z. Win is with the Laboratory for Information and Decision Systems, Massachusetts Institute of Technology, Cambridge, MA 02139. E-mail: moewin@mit.edu

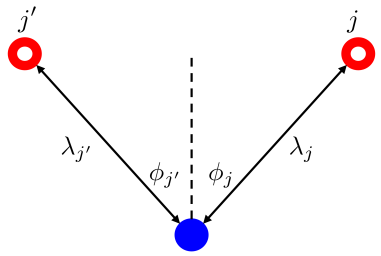

(a) perfect paring

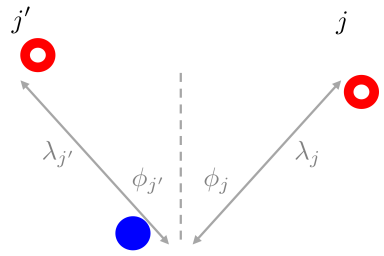

(b) $(\overline{\Delta\lambda}, \overline{\Delta\phi})$-pairing

Fig. 1: Perfect paring between sensor nodes j and $j' = N_\mathrm{b}/2 + j$ is showcased in (a), where $\phi_{j'} = -\phi_j$ and $\lambda_{j'} = \lambda_j$ for $j \in \mathcal{N}_\mathrm{b}^\mathrm{e}$. In this case, the determinant of FIM (3) is equal to its upper bound $\bar{\ell}_\mathrm{d}$ (4). However, in practice, there are discrepancies between the desired network geometry and its actual implementation. Imperfect pairing of nodes is depicted in (b), where $\lambda_{j'} = \lambda_j + \Delta\lambda_j$ and $\phi_{j'} = -\phi_j + \Delta\phi_j$ according to the Definition 1.

Notations: Random variables are displayed in sans serif, upright fonts; their realizations in serif, italic fonts. Vectors and matrices are denoted by bold lowercase and uppercase letters, respectively. For example, a random variable and its realization are denoted by x and x; a random vector and its realization are denoted by $\mathbf{x}$ and $\boldsymbol{x}$, respectively; a random matrix and its realization are denoted by $\mathbf{X}$ and $\boldsymbol{X}$, respectively. Notation $\boldsymbol{A}^\mathrm{T}$ represents the transpose of matrix $\boldsymbol{A}$. For a square matrix $\boldsymbol{A}$, notations $\boldsymbol{A}^{-1}$, $\mathrm{tr}(\boldsymbol{A})$, and $\det(\boldsymbol{A})$ represent its inverse, trace, and determinant, respectively. Notation $\mathrm{diag}(\boldsymbol{A}_1, \boldsymbol{A}_2, \ldots, \boldsymbol{A}_n)$ denotes a block diagonal matrix with the arguments on its main diagonal. Expression $\boldsymbol{A} \succcurlyeq \boldsymbol{B}$ represents that matrix $\boldsymbol{A} - \boldsymbol{B}$ is positive semidefinite.

II. Problem Formulation

Consider a localization network comprised of N_b sensing nodes, with index set $\mathcal{N}_\mathrm{b} = \{1, 2, \ldots, N_\mathrm{b}\}$, at positions $\{\boldsymbol{q}_j\}_{j\in\mathcal{N}_\mathrm{b}}$. Assuming N_b is even, let $\mathcal{N}_\mathrm{b}^\mathrm{e} = \{1, 2, \ldots, N_\mathrm{b}/2\}$. The objective is to estimate the position $\boldsymbol{p}$ of a target of interest via the following ranging measurements

$$\mathbf{r} = [d_1, d_2, \ldots, d_{N_\mathrm{b}}]^\mathrm{T} + \mathbf{w}$$

where $d_j = \|\boldsymbol{p} - \boldsymbol{q}_j\|$ is the distance between the target and j-th node, and $\mathbf{w}$ is a multivariate noise with a normal distribution $\mathcal{N}(\mathbf{0}_{N_\mathrm{b}\times 1}, \mathrm{diag}(\sigma_1, \ldots, \sigma_{N_\mathrm{b}}))$.

Let $\hat{\mathbf{p}}$ be any unbiased estimator of $\boldsymbol{p}$, then under some mild regularity conditions, the Fisher information inequality (FII) [27] states that

$$\mathbb{E}\left\{(\boldsymbol{p} - \hat{\mathbf{p}})(\boldsymbol{p} - \hat{\mathbf{p}})^\mathrm{T}\right\} \succcurlyeq \boldsymbol{J}^{-1}$$

where $\boldsymbol{J}$ is the FIM. In 2D scenarios, $\boldsymbol{J}$ is given by

$$\boldsymbol{J} \triangleq \sum_{j\in\mathcal{N}_\mathrm{b}} \lambda_j \begin{bmatrix} \cos^2(\phi_j) & \cos(\phi_j)\sin(\phi_j) \\ \cos(\phi_j)\sin(\phi_j) & \sin^2(\phi_j) \end{bmatrix}.$$

Here, λ_j is the RII of the j-th node. In particular, λ_j is equal to the signal-to-noise ratio (SNR) of the signal transmitted by the jth node and received by the target in scenarios where the network is synchronized. Symbol ϕ_j represents the relative angle of the j-th node with respect to the target [28].

According to the literature of optimal designs [29, p. 387], there are several criteria for assessing the network geometry that can be written as functions of the eigenvalues of $\boldsymbol{J}^{-1}$. The D-optimality criterion corresponds to the minimization of $\det(\boldsymbol{J}^{-1})$, the minimization of $\mathrm{tr}(\boldsymbol{J}^{-1})$ is the goal of the A-optimality criterion, while the E-optimality criterion aims to minimize the largest eigenvalue of $\boldsymbol{J}^{-1}$. In a 2-D network, $\boldsymbol{J}^{-1}$ is a 2×2 non-singular matrix, and it follows that

$$\mathrm{tr}(\boldsymbol{J}^{-1}) = \frac{\mathrm{tr}(\boldsymbol{J})}{\det(\boldsymbol{J})} \tag{1}$$

and the largest eigenvalue is given by

$$\mathrm{v}(\boldsymbol{J}^{-1}) = \frac{\mathrm{tr}(\boldsymbol{J}) + \sqrt{\mathrm{tr}^2(\boldsymbol{J}) - 4\det(\boldsymbol{J})}}{2}. \tag{2}$$

Due to the considered sensing setup [28], note that $\mathrm{tr}(\boldsymbol{J}) = \sum_{j\in N_\mathrm{b}} \lambda_j$ is not a function of the relative angles and

$$\det(\boldsymbol{J}) = \left(\sum_{j\in N_\mathrm{b}} \lambda_j \cos^2(\phi_j)\right)\left(\sum_{j\in N_\mathrm{b}} \lambda_j \sin^2(\phi_j)\right) - \left(\sum_{j\in N_\mathrm{b}} \lambda_j \cos(\phi_j)\sin(\phi_j)\right)^2. \tag{3}$$

In the following, we characterize the optimal node deployment according to the D-optimality criterion, which is equivalent to maximizing the FIM determinant of (3). Subsequently, we discuss its implications for the A-optimality and E-optimality criteria. Our network design is based on the pairing of nodes as described next. First, notice that $\det(\boldsymbol{J})$ is upper bounded by the first summand in (3) as

$$\det(\boldsymbol{J}) \leqslant \bar{\ell}_\mathrm{d} \triangleq \big(\mathrm{tr}(\boldsymbol{J}) - \Pi\big)\Pi \tag{4}$$

where

$$\Pi \triangleq \sum_{j\in N_\mathrm{b}} \lambda_j \sin^2(\phi_j).$$

If $\phi_j = -\phi_{j+N_\mathrm{b}/2}$ and $\lambda_j = \lambda_{j+N_\mathrm{b}/2}$ for all $j \in \mathcal{N}_\mathrm{b}^\mathrm{e}$, the second summand in (3) vanishes and $\det(\boldsymbol{J})$ becomes equal to its upper bound $\bar{\ell}_\mathrm{d}$ (4) (see Fig. 1a). When the RII of the nodes

are given and equal, this symmetric pattern with respect to the target of interest has been studied in [32]. However, in many applications, such as indoor positioning systems or IoBT, it is *not possible* to deploy the nodes such that $\phi_j = -\phi_{j+N_\mathrm{b}/2}$ and $\lambda_j = \lambda_{j+N_\mathrm{b}/2}$ for all $j \in \mathcal{N}_\mathrm{b}^\mathrm{e}$. Also, in applications such as OoT, the positions of nodes might change due to environmental disturbances such as wind and ocean currents. In this case, $\det(\boldsymbol{J})$ will not be equal to $\bar{\ell}_\mathrm{d}$.

Definition 1: For each node j, consider a node $j' = j+N_\mathrm{b}/2$ such that $\lambda_{j'} = \lambda_j + \Delta\lambda_j$ and $\phi_{j'} = -\phi_j + \Delta\phi_j$. Given $\overline{\Delta\lambda} \geqslant 0$ and $\overline{\Delta\phi} \geqslant 0$, a set of nodes is called $(\overline{\Delta\lambda}, \overline{\Delta\phi})$-*paired*, if nodes can be partitioned into pairs such that $|\Delta\lambda_j| \leqslant \overline{\Delta\lambda}$ and $|\Delta\phi_j| \leqslant \overline{\Delta\phi}$, for $j \in \mathcal{N}_\mathrm{b}^\mathrm{e}$. In the special case $\overline{\Delta\lambda} = \overline{\Delta\phi} = 0$, the nodes are referred to as being *perfectly paired*.

With the above definition, pairs of nodes are constructed such that the absolute value of the difference in their RIIs can be upper bounded by $\overline{\Delta\lambda}$, and the absolute value of the sum of their relative angles is less than $\overline{\Delta\phi}$, see Fig. 1. Next, we study the optimal network geometry for $(\overline{\Delta\lambda}, \overline{\Delta\phi})$-paired nodes.

III. Bounds on the Determinant of FIM for Relaxed Node Deployment

Assuming $(\overline{\Delta\lambda}, \overline{\Delta\phi})$-paired nodes, we will find upper and lower bounds on $\det(\boldsymbol{J})$. These bounds will serve to identify points or regions in which $\det(\boldsymbol{J})$ is maximized, and will help to provide an efficient optimization-based guideline for practical algorithm design as explained in the next section.

The upper bound $\bar{\ell}_\mathrm{d}$ in (4) is concave in Π, and the maximum occurs at $\Pi = \mathrm{tr}(\boldsymbol{J})/2$. Using trigonometric identities it can be seen that the equation $\Pi = \mathrm{tr}(\boldsymbol{J})/2$ is equivalent to $\sum_{j\in\mathcal{N}_\mathrm{b}} \lambda_j \cos(2\phi_j) = 0$. Thus, $\bar{\ell}_\mathrm{d}$ is maximized if it is possible to set $\phi_j = \pm\pi/4$, and the upper bound $\bar{\ell}_\mathrm{d}$ is bounded from above by the *perfect-pairing bound* $\bar{\ell}_\mathrm{d}^* \triangleq (\mathrm{tr}(\boldsymbol{J}))^2/4$. Given a set of $(\overline{\Delta\lambda}, \overline{\Delta\phi})$-paired nodes, in the next theorem, we derive a lower bound on $\det(\boldsymbol{J})$ and bound its distance to $\bar{\ell}_\mathrm{d}$, and also bound the distance of $\bar{\ell}_\mathrm{d}$ with its upper bound $\bar{\ell}_\mathrm{d}^*$.

Theorem 1: Assuming an even number N_b of nodes that admits a $(\overline{\Delta\lambda}, \overline{\Delta\phi})$-pairing according to Definition 1, $\det(\boldsymbol{J})$ is bounded from below by $\underline{\ell}_\mathrm{d} \triangleq \bar{\ell}_\mathrm{d} - \epsilon$, where

$$\epsilon \triangleq \Bigg(\Big| \sum_{j\in\mathcal{N}_\mathrm{b}^\mathrm{e}} \lambda_j \sin^2(\Delta\phi_j)\sin(2\phi_j) + \frac{1}{2}\sum_{j\in\mathcal{N}_\mathrm{b}^\mathrm{e}} \lambda_j \sin(2\Delta\phi_j)\cos(2\phi_j) \Big| + \frac{N_\mathrm{b}\overline{\Delta\lambda}}{4} \Bigg)^2 \tag{5}$$

and $\bar{\ell}_\mathrm{d}$ is the upper bound on $\det(\boldsymbol{J})$ defined in (4). Furthermore, the difference between $\bar{\ell}_\mathrm{d}$ and its upper bound $\bar{\ell}_\mathrm{d}^*$ is not larger than δ, that is $\bar{\ell}_\mathrm{d}^* - \bar{\ell}_\mathrm{d} \leqslant \delta$, where

$$\delta \triangleq \Bigg(\Big| \sum_{j\in\mathcal{N}_\mathrm{b}^\mathrm{e}} \lambda_j \cos^2(\Delta\phi_j)\cos(2\phi_j) + \frac{1}{2}\sum_{j\in\mathcal{N}_\mathrm{b}^\mathrm{e}} \lambda_j \sin(2\Delta\phi_j)\sin(2\phi_j) \Big| + \frac{N_\mathrm{b}\overline{\Delta\lambda}}{4} \Bigg)^2. \tag{6}$$

Proof: To find a lower bound on $\det(\boldsymbol{J})$, we aim to find an upper bound on the last summand of (3) as follows. Using the trigonometric identity and Definition 1 it follows that

$$\sum_{j\in\mathcal{N}_\mathrm{b}} \lambda_j \cos(\phi_j)\sin(\phi_j) = \frac{1}{2}\sum_{j\in\mathcal{N}_\mathrm{b}^\mathrm{e}} \big(\lambda_j \sin(2\phi_j) + \lambda_{j'}\sin(2\phi_{j'})\big). \tag{7}$$

Moreover, using trigonometric identities and Definition 1,

$$\begin{aligned}&\lambda_j \sin(2\phi_j) + \lambda_{j'}\sin(2\phi_{j'}) \\ &= 2\lambda_j \sin(\Delta\phi_j)\big(\cos(2\phi_j)\cos(\Delta\phi_j) + \sin(2\phi_j)\sin(\Delta\phi_j)\big) \\ &\quad + \Delta\lambda_j \sin(2\phi_{j'}).\end{aligned} \tag{8}$$

Combining (7) and (8), using $|\sin(2\phi_{j'})| \leq 1$, and the double-angle trigonometric identity, we obtain

$$\begin{aligned}\Big|\sum_{j\in\mathcal{N}_\mathrm{b}} \lambda_j \cos(\phi_j)\sin(\phi_j)\Big| &\leqslant \Big|\frac{1}{2}\sum_{j\in\mathcal{N}_\mathrm{b}^\mathrm{e}} \lambda_j \sin(2\Delta\phi_j)\cos(2\phi_j) \\ &\quad + \sum_{j\in\mathcal{N}_\mathrm{b}^\mathrm{e}} \lambda_j \sin^2(\Delta\phi_j)\sin(2\phi_j)\Big| + \frac{1}{2}\sum_{j\in\mathcal{N}_\mathrm{b}^\mathrm{e}} |\Delta\lambda_j|.\end{aligned} \tag{9}$$

Using (3), (4), (9), and the paring property, we obtain (5).

Next, we prove (6). As discussed before Theorem 1, $\bar{\ell}_\mathrm{d}$ is concave in Π, and the maximum occurs at $\Pi = \mathrm{tr}(\boldsymbol{J})/2$. Moreover, given $\eta \geqslant 0$, if $\Pi = \mathrm{tr}(\boldsymbol{J})/2 \pm \eta$, that is,

$$\Big|\frac{1}{2}\sum_{j\in\mathcal{N}_\mathrm{b}} \lambda_j \cos(2\phi_j)\Big| = \eta \tag{10}$$

then $\bar{\ell}_\mathrm{d} = \bar{\ell}_\mathrm{d}^* - \eta^2$. Using Definition 1, we have

$$\sum_{j\in\mathcal{N}_\mathrm{b}} \lambda_j \cos(2\phi_j) = \sum_{j\in\mathcal{N}_\mathrm{b}^\mathrm{e}} \big(\lambda_j \cos(2\phi_j) + \lambda_{j'}\cos(2\phi_{j'})\big) \tag{11}$$

also using the sum-to-product and the angle-difference trigonometric identity, similar to (8), it follows that

$$\begin{aligned}&\lambda_j \cos(2\phi_j) + \lambda_{j'}\cos(2\phi_{j'}) \\ &= 2\lambda_j \cos(\Delta\phi_j)\big(\cos(2\phi_j)\cos(\Delta\phi_j) + \sin(2\phi_j)\sin(\Delta\phi_j)\big) \\ &\quad + \Delta\lambda_j \cos(2\phi_{j'}).\end{aligned} \tag{12}$$

By combining (11), (12), and the double-angle trigonometric identity, we obtain

$$\begin{aligned}\frac{1}{2}\sum_{j\in\mathcal{N}_\mathrm{b}} \lambda_j \cos(2\phi_j) &= \sum_{j\in\mathcal{N}_\mathrm{b}^\mathrm{e}} \lambda_j \cos^2(\Delta\phi_j)\cos(2\phi_j) \\ &\quad + \frac{1}{2}\sum_{j\in\mathcal{N}_\mathrm{b}^\mathrm{e}} \lambda_j \sin(2\phi_j)\sin(2\Delta\phi_j) \\ &\quad + \frac{1}{2}\sum_{j\in\mathcal{N}_\mathrm{b}^\mathrm{e}} \Delta\lambda_j \cos(2\phi_{j'}).\end{aligned} \tag{13}$$

Hence, using (10), (13), and since $|\cos(2\phi_{j'})| \leqslant 1$, we obtain the following upper bound

$$\begin{aligned}\eta \leqslant \Big| &\sum_{j\in\mathcal{N}_\mathrm{b}^\mathrm{e}} \lambda_j \cos^2(\Delta\phi_j)\cos(2\phi_j) \\ &+ \frac{1}{2}\sum_{j\in\mathcal{N}_\mathrm{b}^\mathrm{e}} \lambda_j \sin(2\Delta\phi_j)\sin(2\phi_j)\Big| + \frac{N_\mathrm{b}\overline{\Delta\lambda}}{4}\end{aligned} \tag{14}$$

which results in (6). □

Figures 2a and 2b show $\det(\boldsymbol{J})$ as well as its upper and lower bounds derived in Theorem 1 as functions of $\overline{\Delta\lambda}$ and $\overline{\Delta\phi}$, respectively. In the two figures, a scenario with six nodes $N_{\rm b}=6$, $\lambda_1=\lambda_2=\lambda_3=1$, $\phi_1=0$, $\phi_2=\pi/4$, and $\phi_3=\pi/4$ is considered. In Figure 2a, $\lambda_{j+N_{\rm b}/2}=\lambda_j+\overline{\Delta\lambda}$, where $\overline{\Delta\lambda}$ is represented on the X-axis of the figure, and $\phi_{j+N_{\rm b}/2}=-\phi_j+0.01$ for $j\in\mathcal{N}_{\rm b}^{\rm e}$. It can be seen from Fig. 2a that all the bounds are increasing with $\overline{\Delta\lambda}$. This can be attributed to the fact that the SNR increases with $\overline{\Delta\lambda}$. It can also be noticed that the gap between the different bounds increases with $\overline{\Delta\lambda}$. This is because the pairing error is increasing with $\overline{\Delta\lambda}$. In Fig. 2b, $\phi_{j+N_{\rm b}/2}=-\phi_j+\overline{\Delta\phi}$, where $\overline{\Delta\phi}$ is represented on the X-axis of the figure, and $\lambda_{j+N_{\rm b}/2}=\lambda_j+0.1$ for $j\in\mathcal{N}_{\rm b}^{\rm e}$.

The following corollaries discuss the implications of Theorem 1 on the A-optimality and E-optimality criteria. Their proofs are straightforward and follow via (1), (2), and Theorem 1, that are omitted due to the space constraints.

Corollary 1: Under the assumptions of Theorem 1, the $\mathrm{tr}(\boldsymbol{J}^{-1})$ is lower and upper bounded by $\underline{\ell}_{\rm t}\triangleq\mathrm{tr}(\boldsymbol{J})/\bar{\ell}_{\rm d}$ and $\bar{\ell}_{\rm t}\triangleq\mathrm{tr}(\boldsymbol{J})/\underline{\ell}_{\rm d}$, respectively. Here, $\bar{\ell}_{\rm t}-\underline{\ell}_{\rm t}\leqslant(\mathrm{tr}(\boldsymbol{J})\epsilon)/(\underline{\ell}_{\rm d}(\underline{\ell}_{\rm d}+\epsilon))$ and $\underline{\ell}_{\rm t}^{*}+(16\delta)/(\mathrm{tr}(\boldsymbol{J}))^3\geqslant\underline{\ell}_{\rm t}\geqslant\underline{\ell}_{\rm t}^{*}\triangleq 4/\mathrm{tr}(\boldsymbol{J})$.

Corollary 2: Under the assumptions of Theorem 1, the $\mathrm{v}(\boldsymbol{J}^{-1})$ is lower and upper bounded by $\underline{\ell}_{\rm v}\triangleq 0.5\big(\mathrm{tr}(\boldsymbol{J})+2\sqrt{\bar{\ell}_{\rm d}^{*}-\bar{\ell}_{\rm d}}\big)$ and $\bar{\ell}_{\rm v}\triangleq 0.5\big(\mathrm{tr}(\boldsymbol{J})+2\sqrt{\bar{\ell}_{\rm d}^{*}-\underline{\ell}_{\rm d}}\big)$, respectively. Here, $\underline{\ell}_{\rm v}^{*}+\sqrt{\delta}\geqslant\underline{\ell}_{\rm v}\geqslant\underline{\ell}_{\rm v}^{*}\triangleq\mathrm{tr}(\boldsymbol{J})/2$ and, provided $\sqrt{\bar{\ell}_{\rm d}^{*}-\bar{\ell}_{\rm d}}+\sqrt{\bar{\ell}_{\rm d}^{*}-\underline{\ell}_{\rm d}}\neq 0$, we have $\bar{\ell}_{\rm v}-\underline{\ell}_{\rm v}\leqslant\epsilon/\left(\sqrt{\epsilon+\delta}+\sqrt{\delta}\right)$.

IV. Optimization-based relaxed node deployment

In many applications, such as radar and sonar, the target is far away from the nodes. In this case, it might not be possible to encircle the target with nodes, and the range of relative angles for the nodes with respect to the target is constrained. From the D-optimality and the pairing design described in Section II, the optimization problem of finding the optimal network geometry can be stated as follows

$$\begin{aligned}\mathscr{P}_1:\ \underset{\boldsymbol{\lambda}^{\rm e},\boldsymbol{\phi}^{\rm e}}{\text{maximize}}\quad & \det(\boldsymbol{J})\\ \text{subject to}\quad & 0\leqslant\lambda_j\leqslant\bar{\lambda}\,,\qquad \forall j\in\mathcal{N}_{\rm b}^{\rm e}\\ & \iota_1\leqslant\phi_j\leqslant\iota_2\,,\qquad \forall j\in\mathcal{N}_{\rm b}^{\rm e}\end{aligned}$$

where $\iota_1\in\mathbb{R}$, $\iota_2\in\mathbb{R}$, $\bar{\lambda}\in(0,\infty)$, $\boldsymbol{\lambda}^{\rm e}\triangleq[\lambda_1,\lambda_2,\ldots,\lambda_{N_{\rm b}/2}]$, and $\boldsymbol{\phi}^{\rm e}\triangleq[\phi_1,\phi_2,\ldots,\phi_{N_{\rm b}/2}]$. By considering $\boldsymbol{\lambda}^{\rm e},\boldsymbol{\phi}^{\rm e}$ in Problem $\mathscr{P}_1$, we only need to optimize one half of the sensing nodes, whereas the other half is placed such that the entire set of nodes forms a $(\overline{\Delta\lambda},\overline{\Delta\phi})$-pairing according to Definition 1.

As $\det(\boldsymbol{J})$ in (3) is not a straightforward objective for optimization purposes, we will find a relevant optimization program to Problem $\mathscr{P}_1$, which can be efficiently solved. Theorem 1 states that the distance between the lower and upper bounds of $\det(\boldsymbol{J})$ is less than ϵ, and also the distance between the upper bound $\bar{\ell}_{\rm d}$ and its upper bound $\bar{\ell}_{\rm d}^{*}$ is less than δ. Thus, to maximize $\det(\boldsymbol{J})$ we now investigate an optimization program that minimizes ϵ and δ, and maximizes $\bar{\ell}_{\rm d}^{*}$. In fact, for simplicity, we focus on the case where $\iota_1=0$, $\iota_2=\pi/4$, and the upper bound on discrepancies in the relative angles is $\overline{\Delta\phi}\leqslant\pi/4$. In this case, ϵ in (5) and δ in (6) can be bounded from below by $\bar{\epsilon}$ in (15) and $\bar{\delta}$ in (16), respectively, which are given at the bottom of this page. Using (15) and (16), minimizing $\bar{\epsilon}+\bar{\delta}$ is equivalent to minimizing

$$\Upsilon\triangleq\alpha\sum_{j\in\mathcal{N}_{\rm b}^{\rm e}}\lambda_j\cos(2\phi_j)+\beta\sum_{j\in\mathcal{N}_{\rm b}^{\rm e}}\lambda_j\sin(2\phi_j)\tag{17}$$

where $\alpha\triangleq 1+\frac{1}{2}\sin(2\overline{\Delta\phi})$ and $\beta\triangleq\sin^2(\overline{\Delta\phi})+\frac{1}{2}\sin(2\overline{\Delta\phi})$. Also, according to Theorem 1, minimizing $\bar{\epsilon}+\bar{\delta}$ leads to the minimization of the distance between the lower and upper bounds of $\det(\boldsymbol{J})$. Thus, we consider the following optimization program

$$\begin{aligned}\mathscr{P}_2:\ \underset{\boldsymbol{\lambda}^{\rm e},\boldsymbol{\phi}^{\rm e}}{\text{maximize}}\quad & \sum_{j\in\mathcal{N}_{\rm b}^{\rm e}}\lambda_j-\Upsilon\\ \text{subject to}\quad & 0\leqslant\lambda_j\leqslant\bar{\lambda}\,,\qquad \forall j\in\mathcal{N}_{\rm b}^{\rm e}\\ & \iota_1\leqslant\phi_j\leqslant\iota_2\,,\qquad \forall j\in\mathcal{N}_{\rm b}^{\rm e}\,.\end{aligned}$$

Here, by maximizing $\sum_{j\in\mathcal{N}_{\rm b}^{\rm e}}\lambda_j$ we are maximizing $\bar{\ell}_{\rm d}^{*}$, which is an upper bound on $\det(\boldsymbol{J})$, and by minimizing Υ, we are minimizing the distance of $\det(\boldsymbol{J})$ with $\bar{\ell}_{\rm d}^{*}$.

Using the harmonic addition theorem and (17), it follows that

$$\Upsilon=\sqrt{\alpha^2+\beta^2}\sum_{j\in\mathcal{N}_{\rm b}^{\rm e}}\lambda_j\cos\left(2\phi_j+\tan^{-1}\left(-\frac{\beta}{\alpha}\right)\right).\tag{18}$$

Thus, by letting $\zeta_j\triangleq\cos\left(2\phi_j+\tan^{-1}\left(-\frac{\beta}{\alpha}\right)\right)$, the Problem $\mathscr{P}_2$ can be re-written as

$$\begin{aligned}\mathscr{P}_3:\ \underset{\boldsymbol{\lambda}^{\rm e},\boldsymbol{\zeta}^{\rm e}}{\text{maximize}}\quad & \sum_{j\in\mathcal{N}_{\rm b}^{\rm e}}\lambda_j\left(1-\zeta_j\sqrt{\alpha^2+\beta^2}\right)\\ \text{subject to}\quad & 0\leqslant\lambda_j\leqslant\bar{\lambda}\,,\qquad \forall j\in\mathcal{N}_{\rm b}^{\rm e}\\ & \underline{\zeta}\leqslant\zeta_j\leqslant\bar{\zeta}\,,\qquad \forall j\in\mathcal{N}_{\rm b}^{\rm e}\end{aligned}$$

$$\bar{\epsilon}\triangleq\left(\sin^2(\overline{\Delta\phi})\sum_{j\in\mathcal{N}_{\rm b}^{\rm e}}\lambda_j\sin(2\phi_j)+\frac{1}{2}\sin(2\overline{\Delta\phi})\sum_{j\in\mathcal{N}_{\rm b}^{\rm e}}\lambda_j\cos(2\phi_j)+\frac{N_{\rm b}\overline{\Delta\lambda}}{4}\right)^2\tag{15}$$

$$\bar{\delta}\triangleq\left(\sum_{j\in\mathcal{N}_{\rm b}^{\rm e}}\lambda_j\cos(2\phi_j)+\frac{1}{2}\sin(\overline{\Delta\phi})\sum_{j\in\mathcal{N}_{\rm b}^{\rm e}}\lambda_j\sin(2\phi_j)+\frac{N_{\rm b}\overline{\Delta\lambda}}{4}\right)^2\tag{16}$$

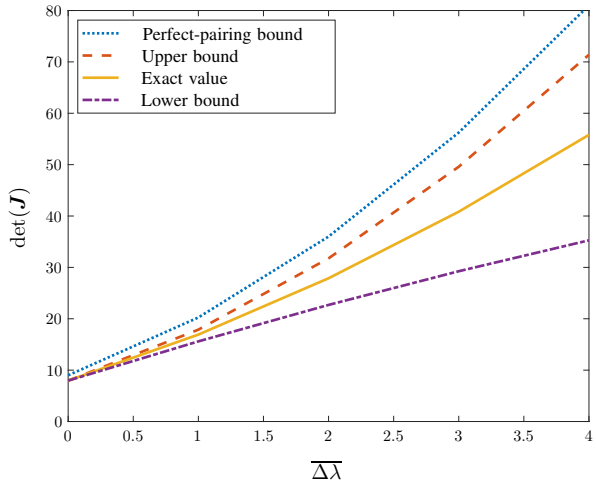

(a) RII

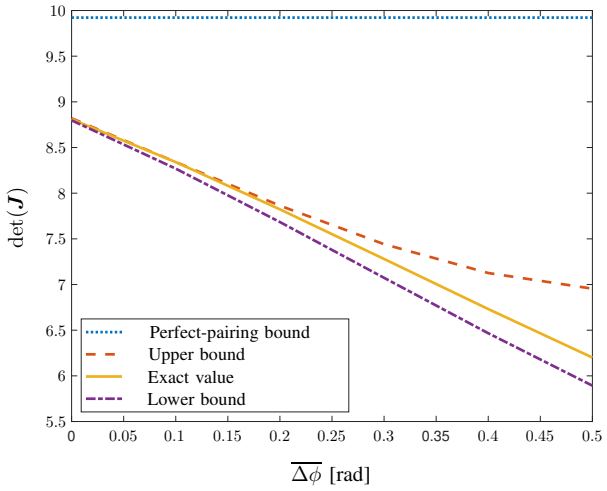

(b) relative angle

Fig. 2: Showcasing the FIM determinant $\det(\boldsymbol{J})$ and its upper $\bar{\ell}_{\rm d}$ and lower $\underline{\ell}_{\rm d}$ bounds derived in Theorem 1 as functions of: (a) $\overline{\Delta\lambda}$, the upper bound on the mismatch in the RII, and (b) $\overline{\Delta\phi}$, the upper bound on the mismatch in the relative angles. The perfect-pairing bound is given by $\bar{\ell}^{*}_{\rm d} = \big(\mathrm{tr}(\boldsymbol{J})\big)^2/4$.

where $\boldsymbol{\zeta}^{\rm e} \triangleq [\zeta_1, \zeta_2, \ldots, \zeta_{N_{\rm b}/2}]$. As $0 \leqslant \overline{\Delta\phi} \leqslant \pi/4$, $\tan^{-1}(-\beta/\alpha) \in [-\tan^{-1}(2/3), 0]$. Also, $0 \leqslant 2\phi_j \leqslant \pi/2$ for all $j \in \mathcal{N}_{\rm b}^{\rm e}$; hence, in $\mathscr{P}_3$, $\bar{\zeta} = 1$, and $\underline{\zeta} = \sin(\tan^{-1}(\alpha/\beta))$. In fact, $\mathscr{P}_3$ is an instance of bilinear programming with efficient solvers given in [29].

A. Special Case: Fixed RIIs

This section presents the special case where the RIIs $\{\lambda_j\}_{j\in\mathcal{N}_{\rm b}}$ are fixed, and we optimize over the relative angles $\{\phi_j\}_{j\in\mathcal{N}_{\rm b}}$. In this case, the Problem $\mathscr{P}_2$ reduces to

$$\mathscr{P}_4: \ \underset{\boldsymbol{\phi}^{\rm e}}{\text{minimize}} \quad \Upsilon$$
$$\text{subject to} \quad \iota_1 \leqslant \phi_j \leqslant \iota_2\,, \qquad \forall j \in \mathcal{N}_{\rm b}^{\rm e}\,.$$

The work in [32] considered this special case, where the nodes are perfectly paired, that is $\overline{\Delta\lambda} = \overline{\Delta\phi} = 0$. Letting $\overline{\Delta\phi} = 0$ in (17), then $\mathscr{P}_4$ reduces to the minimization of $\sum_{j\in\mathcal{N}_{\rm b}^{\rm e}} \lambda_j \cos(2\phi_j)$. By trigonometric identities, it is easy to check that this is equivalent to the criterion derived in [32].

Figure 3 shows $\det(\boldsymbol{J})$ as a function of $\overline{\Delta\phi}$ achieved by the node-deployment method with the perfect-pairing of [32] and the method with $(\overline{\Delta\lambda}, \overline{\Delta\phi})$-pairing proposed in this paper. Here $\lambda_j = 1$ for all $j \in \mathcal{N}_{\rm b}$. A Monte Carlo simulation with 250 independent simulations was performed. We assumed $\phi_j = \phi_j^* + 0.5\,\theta_j\,\overline{\Delta\phi}$ and $\phi_{j+N_{\rm b}/2} = -\phi_j^* - 0.5\,\theta_j\,\overline{\Delta\phi}$ for all $j \in \mathcal{N}_{\rm b}^{\rm e}$, where ϕ_j^* is the optimal node deployment according to either the nominal method of [32] or our design. Also, θ_j, for all $j \in \mathcal{N}_{\rm b}^{\rm e}$, are three independent samples from a truncated normal distribution with mean 1, variance 4, and support set $[0, 1]$. Fig. 3 shows that when $\overline{\Delta\phi}$ tends to zero, our approach has the same performance as the method presented in [32], which is based on perfect-pairing. Also, as $\overline{\Delta\phi}$ increases,

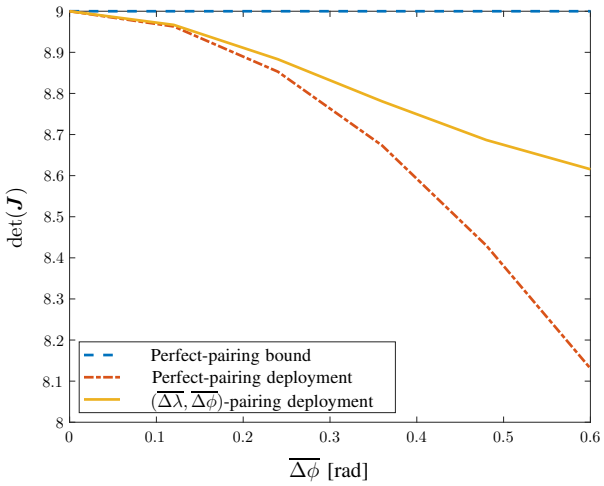

Fig. 3: The FIM determinant $\det(\boldsymbol{J})$ achieved using the node-deployment method with perfect-pairing of [32] and with the proposed $(\overline{\Delta\lambda}, \overline{\Delta\phi})$-pairing method. The perfect-pairing bound is given by $\bar{\ell}^{*}_{\rm d} = \big(\mathrm{tr}(\boldsymbol{J})\big)^2/4$.

the node deployment with $(\overline{\Delta\lambda}, \overline{\Delta\phi})$-pairing outperforms the nominal deployment of [32].

V. Conclusion

We developed a framework for optimal node deployment that accounts for uncertainties in the positions of sensing nodes. In particular, we characterized the upper and lower bounds on the determinant of FIM and identified the gaps between these bounds. We developed a robust node deployment algorithm by solving a bilinear program. Numerical results

showed the performance gain of our algorithm in the D-optimality criterion. We noticed that disturbances in the positions of the sensing nodes could deteriorate the performance of the NLN and demonstrated how the effect of such disturbances is mitigated by our proposed method. The proposed framework sets a basis for the study of robust NLN in the presence of uncertainties in the sensing nodes' positions.

REFERENCES

[1] M. Z. Win, A. Conti, S. Mazuelas, Y. Shen, W. M. Gifford, D. Dardari, and M. Chiani, "Network localization and navigation via cooperation," *IEEE Commun. Mag.*, vol. 49, no. 5, pp. 56–62, May 2011.

[2] A. Conti, F. Morselli, Z. Liu, S. Bartoletti, S. Mazuelas, W. C. Lindsey, and M. Z. Win, "Location awareness in beyond 5G networks," *IEEE Commun. Mag.*, vol. 59, no. 11, pp. 22–27, Nov. 2021.

[3] N. Patwari, J. N. Ash, S. Kyperountas, A. O. Hero, R. L. Moses, and N. S. Correal, "Locating the nodes: Cooperative localization in wireless sensor networks," *IEEE Signal Process. Mag.*, vol. 22, no. 4, pp. 54–69, Jul. 2005.

[4] Newark. (2018) The industrial Internet of Things: Creating intelligent solutions to solve real-world problems. [Online]. Available: https://spectrum.ieee.org/the-industrial-internet-of-things

[5] M. Muro, S. Liu, J. Whiton, and S. Kulkarni, "Digitalization and the American workforce," *Brookings Institute*, 2017.

[6] J. Manyika, M. Chui, M. Miremadi, J. Bughin, K. George, P. Willmott, and M. Dewhurst, "A future that works: AI, automation, employment, and productivity," *McKinsey Global Institute Research, Tech. Rep*, vol. 60, 2017.

[7] Q. D. Vo and P. De, "A survey of fingerprint-based outdoor localization," *IEEE Commun. Surveys Tuts.*, vol. 18, no. 1, pp. 491–506, First quarter 2016.

[8] J. Wang, X. Zhang, Q. Gao, X. Ma, X. Feng, and H. Wang, "Device-free simultaneous wireless localization and activity recognition with wavelet feature," *IEEE Trans. Veh. Technol.*, vol. 66, no. 2, pp. 1659–1669, Feb. 2017.

[9] C. Wen, S. Pan, C. Wang, and J. Li, "An indoor backpack system for 2-D and 3-D mapping of building interiors," *IEEE Geosci. Remote Sens. Lett.*, vol. 13, no. 7, pp. 992–996, Jul. 2016.

[10] D. Balakrishnan and A. Nayak, "An efficient approach for mobile asset tracking using contexts," *IEEE Trans. Parallel Distrib. Syst.*, vol. 23, no. 2, pp. 211–218, Feb. 2012.

[11] E. Paolini, A. Giorgetti, M. Chiani, R. Minutolo, and M. Montanari, "Localization capability of cooperative anti-intruder radar systems," *EURASIP J. Adv. Signal Process.*, vol. 2008, Apr. 2008.

[12] M. Driusso, C. Marshall, M. Sabathy, F. Knutti, H. Mathis, and F. Babich, "Vehicular position tracking using LTE signals," *IEEE Trans. Veh. Technol.*, vol. 66, no. 4, pp. 3376–3391, Apr. 2017.

[13] H. Liu, F. Sun, B. Fang, and X. Zhang, "Robotic room-level localization using multiple sets of sonar measurements," *IEEE Trans. Instrum. Meas.*, vol. 66, no. 1, pp. 2–13, Jan. 2017.

[14] G. Zhan and W. Shi, "LOBOT: Low-cost, self-contained localization of small-sized ground robotic vehicles," *IEEE Trans. Parallel Distrib. Syst.*, vol. 24, no. 4, pp. 744–753, Apr. 2013.

[15] P. Barrios, M. Adams, K. Leung, F. Inostroza, G. Naqvi, and M. E. Orchard, "Metrics for evaluating feature-based mapping performance," *IEEE Trans. Robot.*, vol. 33, no. 1, pp. 198–213, Feb. 2017.

[16] R. Di Taranto, S. Muppirisetty, R. Raulefs, D. Slock, T. Svensson, and H. Wymeersch, "Location-aware communications for 5G networks: How location information can improve scalability, latency, and robustness of 5G," *IEEE Signal Processing Magazine*, vol. 31, no. 6, pp. 102–112, 2014.

[17] S. Bartoletti, A. Conti, and M. Z. Win, "Device-free counting via wideband signals," *IEEE J. Sel. Areas Commun.*, vol. 35, no. 5, pp. 1163–1174, May 2017.

[18] X. Ying, S. Roy, and R. Poovendran, "Pricing mechanisms for crowd-sensed spatial-statistics-based radio mapping," *IEEE Trans. on Cogn. Commun. Netw.*, vol. 3, no. 2, pp. 242–254, Jun. 2017.

[19] R. Estrada, R. Mizouni, H. Otrok, A. Ouali, and J. Bentahar, "A crowd-sensing framework for allocation of time-constrained and location-based tasks," *IEEE Trans. Services Comput.*, vol. PP, no. 99, pp. 1–1, Jul. 2017.

[20] A. Conti, S. Mazuelas, S. Bartoletti, W. C. Lindsey, and M. Z. Win, "Soft information for localization-of-things," *Proc. IEEE*, vol. 107, no. 11, pp. 2240–2264, Nov. 2019.

[21] L. Chen, S. Thombre, K. Järvinen, E. S. Lohan, A. Alén-Savikko, H. Leppäkoski, M. Z. H. Bhuiyan, S. Bu-Pasha, G. N. Ferrara, S. Honkala, J. Lindqvist, L. Ruotsalainen, P. Korpisaari, and H. Kuusniemi, "Robustness, security and privacy in location-based services for future IoT: A survey," *IEEE Access*, vol. 5, pp. 8956–8977, Apr. 2017.

[22] M. Z. Win, F. Meyer, Z. Liu, W. Dai, S. Bartoletti, and A. Conti, "Efficient multi-sensor localization for the Internet of Things," *IEEE Signal Process. Mag.*, vol. 35, no. 5, pp. 153–167, Sep. 2018.

[23] S. D'oro, L. Galluccio, G. Morabito, and S. Palazzo, "Exploiting object group localization in the Internet of Things: Performance analysis," *IEEE Trans. Veh. Technol.*, vol. 64, no. 8, pp. 3645–3656, Aug. 2015.

[24] A. A. Saucan and M. Z. Win, "Information-seeking sensor selection for ocean-of-things," *IEEE Internet Things J*, vol. 7, no. 10, pp. 10 072–10 088, 2020.

[25] B. Teague, Z. Liu, F. Meyer, A. Conti, and M. Z. Win, "Network localization and navigation with scalable inference and efficient operation," *IEEE Trans. Mobile Comput.*, vol. 21, pp. 1–18, 2022, to appear.

[26] T. Abdelzaher, N. Ayanian, T. Basar, S. Diggavi, J. Diesner, D. Ganesan, R. Govindan, S. Jha, T. Lepoint, B. Marlin *et al.*, "Toward an Internet of battlefield things: A resilience perspective," *Computer*, vol. 51, no. 11, pp. 24–36, 2018.

[27] M. Z. Win, Y. Shen, and W. Dai, "A theoretical foundation of network localization and navigation," *Proc. IEEE*, vol. 106, no. 7, pp. 1136–1165, Jul. 2018, special issue on *Foundations and Trends in Localization Technologies*.

[28] M. Z. Win, W. Dai, Y. Shen, G. Chrisikos, and H. V. Poor, "Network operation strategies for efficient localization and navigation," *Proc. IEEE*, vol. 106, no. 7, pp. 1224–1254, Jul. 2018, special issue on *Foundations and Trends in Localization Technologies*.

[29] S. Boyd and L. Vandenberghe, *Convex Optimization*. Cambridge, UK: Cambridge University Press, 2004.

[30] C. Yang, L. Kaplan, and E. Blasch, "Performance measures of covariance and information matrices in resource management for target state estimation," *IEEE Trans. Aerosp. Electron. Syst.*, vol. 48, no. 3, pp. 2594–2613, 2012.

[31] E. Tzoreff and A. J. Weiss, "Path design for best emitter location using two mobile sensors," *IEEE Trans. Signal Process.*, vol. 65, no. 19, pp. 5249–5261, Oct. 2017.

[32] M. Sadeghi, F. Behnia, and R. Amiri, "Optimal sensor placement for 2-D range-only target localization in constrained sensor geometry," *IEEE Trans. Signal Process.*, vol. 68, pp. 2316–2327, 2020.

[33] S. Martínez and F. Bullo, "Optimal sensor placement and motion coordination for target tracking," *Automatica*, vol. 42, no. 4, pp. 661–668, Apr. 2006.

[34] S. Zhao, B. M. Chen, and T. H. Lee, "Optimal sensor placement for target localisation and tracking in 2D and 3D," *Int. J. Control*, vol. 86, no. 10, pp. 1687–1704, 2013.

[35] A. N. Bishop, B. Fidan, B. D. Anderson, K. Doğançay, and P. N. Pathirana, "Optimality analysis of sensor-target localization geometries," *Automatica*, vol. 46, no. 3, pp. 479–492, Mar. 2010.

[36] Y. Shen and M. Z. Win, "Energy efficient location-aware networks," in *Proc. IEEE Int. Conf. Commun.*, Beijing, China, May 2008, pp. 2995–3001.

[37] W. Meng, L. Xie, and W. Xiao, "Optimality analysis of sensor-source geometries in heterogeneous sensor networks," *IEEE Trans. Wireless Commun.*, vol. 12, no. 4, pp. 1958–1967, Apr. 2013.

[38] K. Ho and L. M. Vicente, "Sensor allocation for source localization with decoupled range and bearing estimation," *IEEE Trans. Signal Process.*, vol. 56, no. 12, pp. 5773–5789, 2008.

[39] F. Zabini and A. Conti, "Inhomogeneous Poisson sampling of finite-energy signals with uncertainties in $\mathbb{R}^d$," *IEEE Trans. Signal Process.*, vol. 64, no. 18, pp. 4679–4694, Sep. 2016.

[40] S. Van de Velde, G. Abreu, and H. Steendam, "Bayesian CRLB for hybrid ToA and DoA based wireless localization with anchor uncertainty," in *WPNC'15*, 2015.